A R C H I V E O F M E C H A N I C A L E N G I N E E R I N G

VOL. LXIV 2017 Number 2

DOI: 10.1515/meceng-2017-0016

Key words: energy harvesting, rain, piezoelectric material, renewable energy, mechanical vibration

ROMEO DI LEO[1], *MASSIMO VISCARDI*[1], *FRANCESCO PAOLO TUCCINARDI*[2], *MICHELE VISONE*[3]

NUMERICAL MODELLING OF A PIEZO ROOF HARVESTING SYSTEM: THE RIGHT COMPONENT SELECTION

The present work focuses on a first study for a piezoelectric harvesting system, finalized to the obtaining of electrical energy from the kinetic energy of rainy precipitation, a renewable energy source not really considered until now. The system, after the realization, can be collocated on the roof of an house, configuring a "Piezo Roof Harvesting System". After presenting a state of art of the harvesting systems from environmental energy, linked to vibrations, using piezoelectric structures, and of piezoelectric harvesting systems functioning with rain, the authors propose an analysis of the fundamental features of rainy precipitations for the definition of the harvesting system. Then, four key patterns for the realization of a piezoelectric energy harvesting system are discussed and analysed, arriving to the choice of a cantilever beam scheme, in which the piezoelectric material works in 31 mode. An electro-mechanical model for the simulation of performance of the unit for the energetic conversion, composed of three blocks, is proposed. The model is used for a simulation campaign to perform the final choice of the more suitable piezoelectric unit, available on the market, which will be adopted for the realization of the "Piezo Roof Harvesting System".

1. Introduction

Today, the topic of energy is a crucial point for the future development of the human society. Humanity needs an increasing quantity of energy in the future and the interesting estimation of Energy Outlook of Energy Information Administration EIA quantifies a boost of +55% for the worldwide consumption of energy in the next thirty years [1]. All scientific community agrees about the idea that conventional sources of energy will finish a day. It is no easy to foresee this day and besides it

[1] *Department of Industrial Engineering – Aerospace section, University of Naples "Federico II", Naples – Italy. Emails: romeodileo@gmail.com , maviscar@unina.it*

[2] *Promete S.r.l., Viale Kennedy 5, 80125 – Naples – Italy*

[3] *Blue Design S.r.l., Via Coroglio 57, 80124 – Naples – Italy*

is a strong challenge to find new energy sources able to override the conventional ones.

In this scenario, there is an increasing interest for renewable energy sources as wind and solar energy, which are candidates as future potential contribute for the reduction of consumptions of conventional energy sources or for the complete substitution of them.

Instead, the present paper explores the use of another renewable energy source not really considered until now. The proposed work is focused on meteoric precipitations for the energy production and particularly on the atmospheric phenomena of rain.

Rain falls from the clouds' level, gaining a constant limit velocity of fall when gravity force is equilibrated by the sum of the resistant force, generated from viscous friction, and by the Archimedes pushing force. In this manner, raindrops have a kinetic energy. The final aim is to convert this kinetic energy in the electric one for harvesting energy from the environment.

The use of the environmental energy source of rain pursues a potential advantage as a green production of energy from a new, not conventional, energy source of renewable type but above all an advantage linked to the recent development of MEMS and intelligent systems. This development has carried to a wide use of autonomous sensors. In this field, the recovery of energy from rain can bring the great advantage of feeding autonomous sensors in applications where other energy sources are not available.

In the present work, the result of converting energy from raindrops is pursued through the use of piezoelectric materials. In a particular manner, flexible piezoelectric materials are interesting for power harvesting, because they are able to withstand great strains. Larger strains give a major quantity of mechanical energy for the conversion to electrical energy.

In literature, a lot of research works about the conversion of environmental energy, linked to vibrations, using piezoelectric, are present. A fundamental point to gain a better conversion of mechanical energy in the electric one is the choice of the type of piezoelectric material. Lee, He, Wu and Shih [2] affirm that although piezoceramic materials PZT are widely used in power harvesting field, they present some problematic aspects. In fact, PZT materials are very brittle and this property carries strong limitations in the strain which they can sustain without damages. In a particular way, PZT are sensitive to the propagation of the fatigue under a cycle of load, characterized by a high frequency. To override these limitations of PZT piezoelectric material, a new class of more flexible piezoelectric material was developed. Poly-vinylidene-fluoride PVDF is a polymeric piezoelectric material with great flexibility in comparison to PZT [2].

There are many research works in literature about the topic of a piezoelectric harvesting system for the conversion of environmental energy, linked to vibrations. Lee, Joo, Han, Lee and Koh [3] test a PVDF film coated with poly/poly electrodes. PVDF film works from 10 Hz to 1 MHz without the presence of electrode

damage and it obtain an increasing capacity to harvest power during its lifespan. Mohammadi, Khan and Cass [4] study the power generation ability of piezoelectric lead zirconate titanate fibres composites. They highlight that thicker fibrous plates present larger displacements of fibres and samples with smaller diameter of fibres have the highest d_{33} piezoelectric coefficient and lowest dielectric constant, which are both contributes for a more power conversion and consequently for a more efficient harvesting systems.

Sodano, Lloyd, Park and Inman in their works perform a compare on the efficiency of three different types of piezoelectric materials [5–7]. Classical PZT, macro-fibre composite MFC and a quick pack actuator are considered. Each type of material is excited at resonance, subjected to a 0–500 Hz chirp and then each material is subjected to random vibrations. They find that efficiency of PZT is better than other two systems in all conditions, resonance, chirp and random vibrations.

Besides the choice of the more adequate material, another method of improving the energy converted by a piezoelectric harvesting system is the use of a more efficient coupling mode. There are two coupling modes, 31 mode and 33 mode. In the first one, the force is applied to the piezoelectric material in a perpendicular direction to the poling orientation. In the second mode the direction of applied force and of poling is the same [5–7]. The influence of coupling mode is well described by Baker, Roundy and Wright [8]. Authors analyse alternative geometries for increasing power density in vibration energy scavenging for wireless sensor networks. They load up a cantilever configuration, working in 31 mode, with a stack configuration, working in 33 mode, with the same small force. Authors find the result that a cantilever configuration produces more power (two orders of magnitude) than a stack configuration, subjected to the same force. Stack configuration is more robust and it has a greater coupling coefficient, but it is less productive because the stack has an elevated mechanical stiffness. For this reason, strains of stack configuration are small. In conclusion for small loads, for low level of vibrations the 31 mode of cantilever configuration produces best performances in the energy conversion [8].

Platt, Farritor and Haider [9] study performance of an energy harvesting system, characterized by a stack configuration. One hundred and forty-five PZT wafers are mechanically stacked in series but they are electrically linked in a parallel manner, and this configuration is compared with monolithic PZTs of the same geometry.

Another configuration of piezoelectric materials in an harvesting energy system is given by multiple piezoelectric patches linked to the system. Many harvesting systems present a single piezoceramic working in a bending mode, this configuration is indicated as unimorph. Bimorph configuration is characterized by two bonded piezoelectric patches working in a bending way. Ng and Liao [10] compare a unimorph configuration with two bimorph schemes. Each bimorph scheme is composed by two piezoelectric patches where each piezoelectric is bonded to each face of a metallic layer in a sandwich model. In the first bimorph the two piezoelctric patches are electrically linked in series, in the second one they are

electrically connected in a parallel way. The comparison shows that the unimorph scheme has the highest generation of power under low load resistance and excitation frequencies. Instead, under medium load resistance and frequencies the parallel bimorph configuration achieves best results and under high load resistance and frequencies the parallel scheme has the highest power output.

Besides, many geometries are been analyzed for the cantilever design to suit in a better way to the energy harvesting applications. For example, Roundy [11], Benasciutti, Brusa, Moro, and Zelenika [12] study a piezoelectric trapezoidal shaped cantilever beam. Mateu and Moll [13] in their study about optimum piezoelectric bending beam structures for energy harvesting, using shoe inserts, analyze a triangular shaped piezoelectric element. Mossi, Green, Ounaies and Hughes [14] in the study on geometrical effects for an harvesting energy system, using a thin unimorph pre-stressed bender, propose an arc shaped geometry.

Also harvesting systems with circular shaped piezoelectric elements are been studied. Ericka, Vasic, Costa, Poulin and Tliba [15] use a circular brass layer with a circular PZT layer bonded to its surface, following a unimorph scheme. Kim, Clark and Wang [16, 17] present an analysis and an experimental study on a piezoelectric energy harvesting with a clamped circular plate.

Many of the researches in the last years are also focused on improving the efficiency of piezoelectric circuitry and energy removal techniques as in [18, 19]. Premount [20] highlights the importance of improving the difference between the consumption of energy by electronics used for storing the harvested energy and the capability of generation of the energy harvesting system.

Previous rows show that in literature are present a lot of research works about the conversion of environmental energy, linked to vibrations, using piezoelectric structures, but there are very few works on the topic of a piezoelectric harvesting system functioning with rain. Guigon, Chaillout, Jager and Despesse [21] propose a theoretical study on a possible harvesting raindrop energy system based on a polymeric piezoelectric bands with a length of 100 mm and a width of 3 mm, supported on both the ends. The same authors in another paper [22] complete the study, presenting an experimental work on the piezoelectric system of energy conversion from rain. Biswas, Islam, Sarkar, Desa, Khan and Huq [23] analyze the solution already proposed by the work of Guigon, Chaillout, Jager and Despesse, evaluating the application of this system in the Bangladesh region where the monsoon produces massive rainfall from June to September.

The present work focuses its attention on the proposal of the idea of a "Piezoelectric Shingle" as a new energy harvesting system, based on raindrops. The paper presents a preliminary theoretical and simulative study for the system. The final aim is the conversion of the mechanical kinetic energy of a meteoric precipitation as the rain to electrical energy. The new studied harvesting system results different from the device of Guigon, Chaillout, Jager and Despesse [21, 22], adopting a completely different constructive scheme. In fact, the studied system isn't based on long piezoelectric wires of the Guigon's solution. Besides, the final aim of the

research activity will be the presentation of a finite harvesting system, inserted in a shingle for roof, for this reason the name "Piezoelectric Shingle". The present paper, after a preliminary treatment about the potential features of rainy phenomena interesting for an energy harvesting system, analyzes some basic conceptual ideas for the proposition of a Piezoelectric Shingle. Having selected a conceptual idea, the paper presents an electro-mechanical model, finalized to a simulative methodology for the estimation of performances, given by a piezoelectric unit, stroke by a raindrop.

The electro-mechanical model is used for a simulative study with the final aim of the definition and the choice of the piezoelectric unit, which presents the best performance in an energy harvesting system, based on impacts of raindrops as the Piezoelectric Shingle. This study is the first theoretical and simulative step for a next work with experimental tests in laboratory for the proposed system and for a future final realization of the Piezoelectric Shingle.

2. Features of rainy precipitations interesting for the energy harvesting system

The final aim of the research is the creation of a new piezoelectric device, able to convert the mechanical kinetic energy of rain to electrical energy. For this reason are fundamental two parameters of rainfall: the mass of water and the final limit velocity of fall.

Clearly we are not interested simply in the total mass of water of a rainfall (measured in mm of water/m^2), but it is also important to know each share of this mass which falls with a given final limit velocity. The final limit velocity is related to the diameter of a raindrop. By this preliminary considerations, the fundamental parameters of raindrop for the research project are:

1. the dimension of raindrop (expressed by the value of its diameter),
2. the limit velocity of the drop.

For the first point, it's a focal point to define a distribution law between dimension of raindrops and the nature of rainfall. For this reason, the authors conducted a revision of the state of art in the scientific literature available. In 40's years of the past century, Marshall and Palmer realize experimental measures, using coloured filters of paper [24]. Authors correlate these measures with measures obtained with a radar by Marshall, Langille and Palmer [25]. Considering these results, they affirm that in the proximity of the ground the distribution of the medium dimension of raindrops can be presented by a simple equation proposed by authors:

$$N = (N_0 e^{-\Lambda D})\delta D(1) \tag{1}$$

where: N is the number of drops with diameter inside the interval $[D, D + \delta D]$ in a unitary volume, D is the diameter of the drop, N_0 is an asymptotic value for

diameter D which tends to 0. This parameter is experimentally estimated by authors and it is evaluated equal to 0.08 cm^{-4}. Λ consider the relation with the intensity R (mm/hr.) of the rain $\Lambda = 41R^{-0.21}$ cm^{-1}. This equation is an evolution of the model previously proposed by Laws and Parsons [26] (Fig. 1).

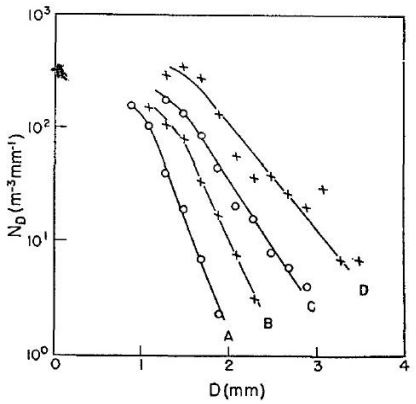

Fig. 1. Curves of Laws and Parsons in a matching with experimental data [26]

Ryde [27], develops the model of Marshall and Palmer, introducing the limit velocity of raindrops. He obtains curves of distribution which link the contribution to the mass of water, generated by drops of a defined diameter. These curves are parameterized in function of the intensity of rainfall (mm/hr.) and they present a "bell shape" (Fig. 2).

The maximum of these curves are approximately distributed on an hyperbolic curve.

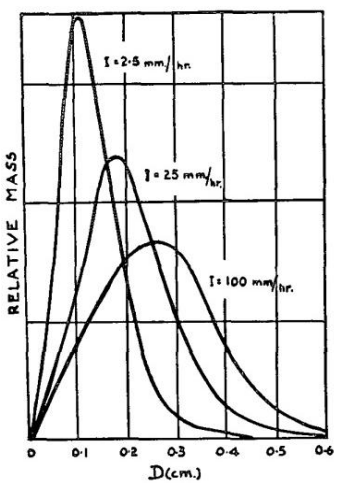

Fig. 2. Ryde's curves about the distribution of raindrops

Best [28] presents a summary and a comparison about all works on the topic and results obtained. After the study of Marshall and Palmer other researches have been conducted to improve the method. Sekhon and Srivastava [29] in 1971 conduct an analysis based on a great number of experimental observations, performed with a Doppler radar. For the curves of Marshall and Palmer they identify a new value of intercept with axis $D = 0$ and this value appears increasing with the parameter R.

Willis in 1984 [30] analyses more than one hundred sets of experimental data, obtained by the methodology of the optical spectroscopy. He normalizes dimensional distributions and find that their trend deviates from the exponential tendency. The author considers five types of functions to gain a best fit to the data: three exponential functions (as Marshall-Palmer type) and two are a "gamma distribution" type. One of the "gamma distribution" gains the best result about the fitting to the experimental data [30]. In this way, he proposes a modification to the widely used Marshall and Palmer method.

In the subsequent curves, a comparison is proposed and the behaviour of new model (Fig. 3a) is better than that of Marshall and Palmer (Fig. 3b), which present a good matching with observed data for raindrops of medium size, but it separates oneself by experimental data for greater or smaller raindrops [30].

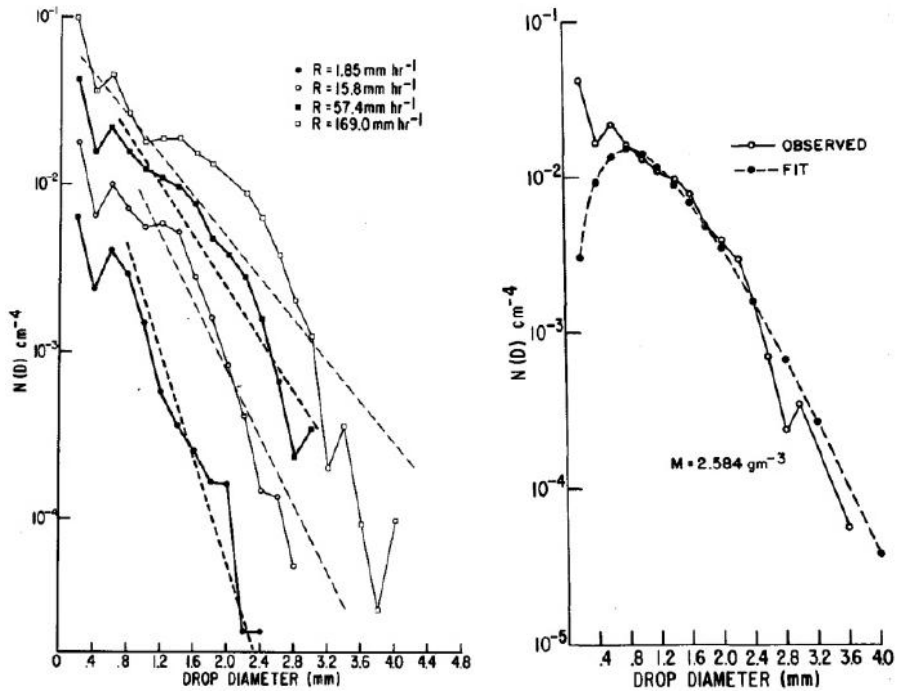

(a) (b)

Fig. 3. Comparison between experimental data and: a) Marshall and Palmer curves for different level of rain rate, b) Marshall and Willis curve

In Israel, Feingold and Levin [31] in 1986 carry out two years of measures about the dimensional distribution of raindrops. They confirm that experimental data can be described in a better manner by a not exponential function. They identify a lognormal distribution with a suitable choice of parameters as a better choice than an exponential one (as the equation of Marshall and Palmer). Besides, this description presents the advantage of a physical meaning for their parameters.

In 90's years Sempere Torres, Porra and Creutin [32] demonstrate that it is possible to find an unifying frame for the parameterization of the distribution for the size of raindrops (rainDrop Size Distribution – DSD). This distribution presents all features of a "law of scale". The same authors in 1998 subsequently confirm this idea with a greater number of experimental experiences. The "law of scale" is clearly function of diameter of raindrop D and of rain rate R. Following the formalism of "laws of scale", the DSD can be expressed as [33]:

$$N(D, R) = R^{\alpha} g(D/R^{\beta}) \tag{2}$$

where: $N(D, R)$ ($\mathrm{mm}^{-1}\mathrm{m}^{-3}$) is the rainDrop Size Distribution – DSD, expressed as a function of diameter of the sphere D (mm) equivalent to the raindrop and the rain rate R ($\mathrm{mm\,h}^{-1}$), α and β are the "exponents of scale" (not dimensional), $g(x)$ is the general distribution of dimensions of raindrops, expressed in function of the scaled diameter of raindrops $x = D/R^{\beta}$.

In accordance with the common practice, the rain rate R is generally considered as the reference variable, but every macroscopic variable of rain can be used for this aim (for example the factor of radar reflectivity Z). It is fundamental to highlight that values of α and β and the shape and dimensions of $g(x)$ depend on the choice of the reference variable, but they are independent from its value [33].

At the beginning of the present section we highlighted that the second fundamental parameter of raindrop for the research project is its limit velocity. The first measures about limit velocity were conducted in 70's years, when in wind gallery the limit velocity of drops of water was measured in saturated air for different number of Reynolds (0,2–200). Beard and Pruppacher (1969) measure the dependence of final velocity by Reynolds number of airflow. They highlight the difference of this final velocity from that of a classical Stokes condition (low Reynolds numbers) [34].

For a rigid sphere in Stokes condition the drag force is:

$$D_s = 6\pi a \eta \eta V_{\infty} \tag{3}$$

where: a is the radius of the rigid sphere, η is the dynamic viscosity, and V_{∞} is the limit velocity.

The value of D_s can be used to obtain a not-dimensional graph of real drag force on the raindrop, dividing the measured value of drag force D to the theoretical value D_s. The ratio D/D_s is the inverse ratio of V_s/V.

Measuring experimentally this last ratio it is possible to evaluate the drag coefficient C_D, which is required for a prevision of the limit velocity:

$$V_\infty = \left(\frac{16}{3}\right)\left(\frac{g(\rho_s - \rho_m)}{\eta}\right)\left(\frac{a^2}{C_D R}\right) \tag{4}$$

with ρ_s and ρ_m, respectively, the density of the water drop and air (environment in which raindrop fall).

The subsequent image (Fig. 4) shows the estimation of C_D, based on experimental measures in function of Reynolds number in a comparison with the theories of Stokes and Oseen for the velocity of fall.

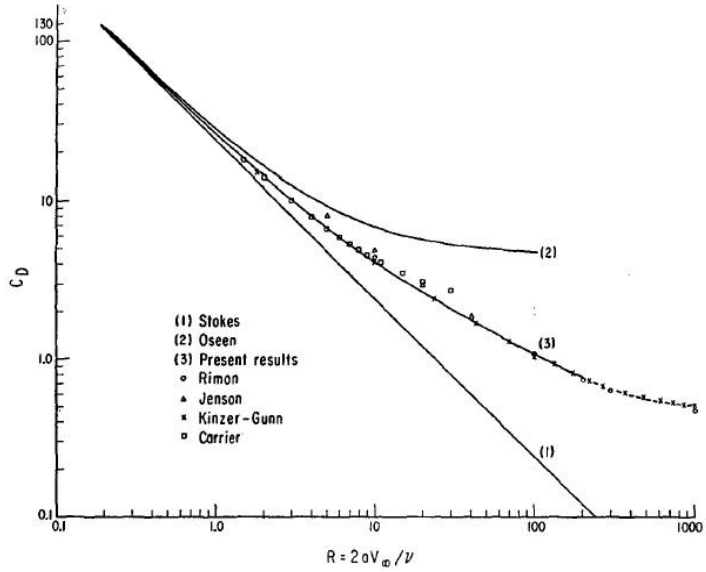

Fig. 4. Measured drag coefficient in a comparison with the results of theories of Stokes and Oseen

This measure through the Reynolds number depends on many physical parameters (diameter of the drop, temperature, humidity and atmospheric pressure). This measure is a useful manner to estimate the limit velocity. In fact, the subsequent quantity is a function only of environmental parameters and raindrop's diameter:

$$C_D R^2 = \left(\frac{32}{3}\right) a^3(\rho_s - \rho_m)\left(\frac{\rho_m g}{\eta^2}\right) \tag{5}$$

Having assigned the value of ρ_s, ρ_m and dynamic viscosity η (function of humidity and temperature) and the raindrop's radius a, it is possible to estimate the Reynols number, inverting the previous expression. In this way, using the known value of C_D and R, it is possible to estimate the limit velocity with the expression

$$V_\infty = \frac{R\eta}{2\rho_m a}. \tag{6}$$

Fig. 5 reports some estimations, made with this technique [34].

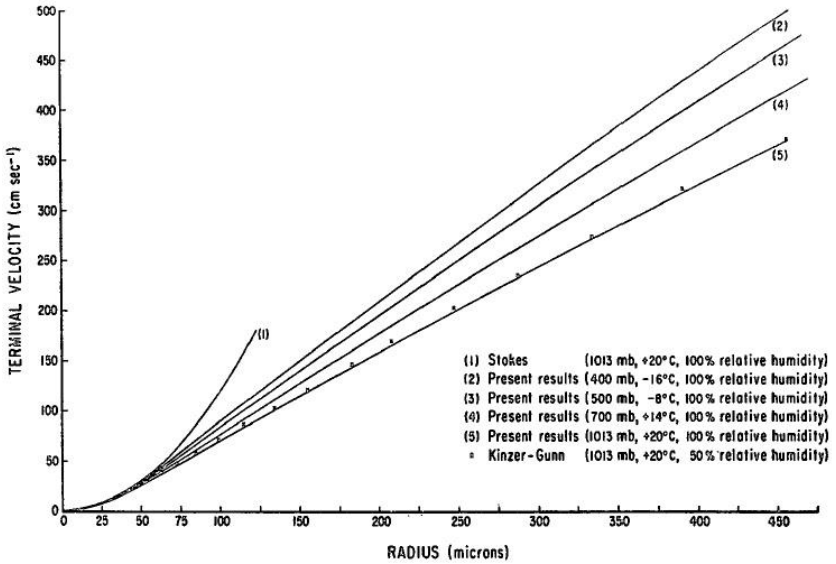

Fig. 5. Limit velocity of raindrops calculated with the procedure presented by Beard and Pruppacher

In a rainy phenomena, not all drops fall effectively at their limit velocity. Recent use new techniques for the measure of the falling drops, show that some drops have a limit velocity of one order of magnitude greater than the expected limit velocity [35]. These drops, called "Super-terminal", carry to an increase of the real energy available against the expected one. For this reason, in the case of an harvesting application, these "Super-terminal drops" can be neglected in the energy estimation in a first approximation.

In the present work, to estimate the limit velocity of raindrops we use the relation, obtained by Guigon R. in 2006 that considers weight (W), viscous friction (R) and Archimedes' push (A) as forces acting on the raindrop [19]. Solving the second equation of dynamic

$$\vec{A} + \vec{W} + \vec{R} = m\vec{a} \tag{7}$$

it is possible to calculate the velocity of a drop in function of its height of fall

$$V(H) = \frac{1}{\alpha}\sqrt{1 - 4e^{-H\alpha b + a + bA}}, \tag{8}$$

with

$$m = \rho_{water}\frac{\pi D^3}{6}; \quad m' = \rho_{air}\frac{\pi D^3}{6}$$

$$k = \frac{1}{8}\rho_{air}\pi D^2 C_D; \quad \mu = \frac{m - m'}{m}$$

and

$$\alpha = \sqrt{\frac{k}{\mu m g}}; \quad a = \ln \frac{1 + \alpha V_{init}}{1 - \alpha V_{init}}$$

$$b = 2\alpha\mu g; \quad A = \frac{-2\ln(e^a + 1)}{b}.$$

The third fundamental feature of rainy precipitation, interesting for an energy harvesting system, is the annual quantity of water fallen in a region. Fig. 6 shows that the region with the greatest annual rainfall (measured as mm/year for every on a square meter) are located in South America, Africa and South-east of Asia (regions of monsoons) with an annual precipitation of about 3000 mm/year. In a detail about Italy, Alpine arch and Apennines ridge are the zones with the greatest annual rainfall (about 1500 mm/year).

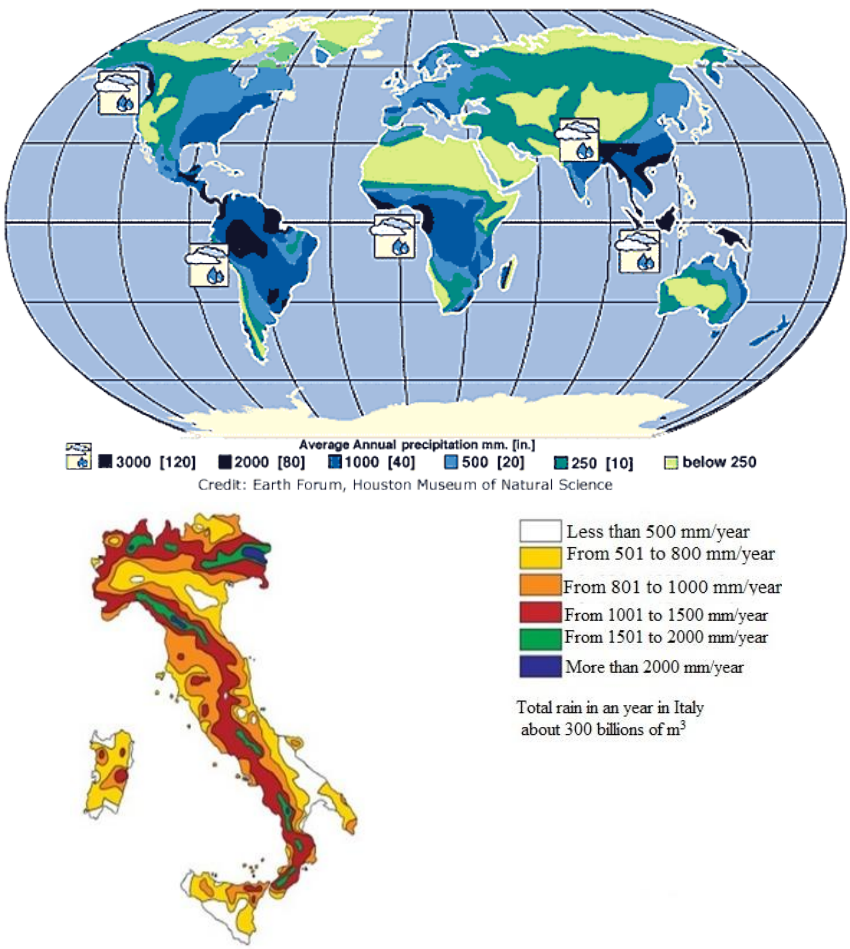

Fig. 6. Annual rainfall in the world and in Italy (mm/a)

Clearly, the system proposed in the present study presents a more potentiality in the region with high annual rainfall with a consequent higher temporal density of energy. All considerations about features of rain, interesting to the energy harvesting system, exposed in the rows of this paragraph will be useful not only for the study of the system but also for an analysis about economic, social and environmental impact of the proposed piezoelectric energy harvesting system. This analysis of impact will be performed in a new future paper after the conclusion of the research activity.

3. Key patterns for a piezoelectric energy harvesting system

Some key patterns for the realization of a piezoelectric energy harvesting system, using rainfall, have been evaluated. The first ideal pattern contemplate the implementation of a piezoelectric patch, bonded by a glue to a membrane. The membrane has a fixed constrain on its four edges (Fig. 7).

The membrane subjected to the loads, generated by impacts of raindrops with its surface, generates a deformation of the membrane and consequently of the bonded piezoelectric patch.

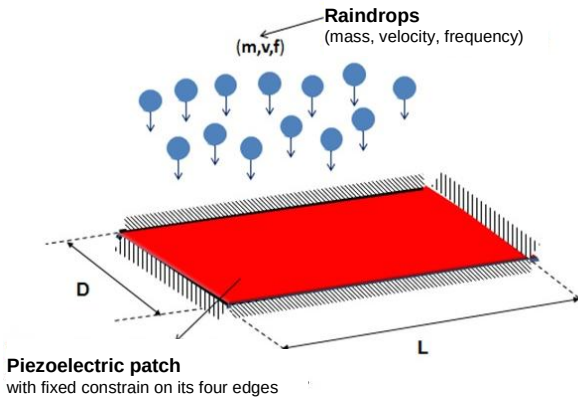

Fig. 7. Ideal concept No.1

The second key patter is based on a piezoelectric stack, which support a collector plate for raindrops. The edges of the plate are free and the only constrained region is the linking interface between the plate and the piezoelectric stack. This pattern follows the conceptual scheme of a piezoelectric scale. In Fig. 8, the second patter is depicted with a spring K_p, representing the stiffness of the piezoelectric stack.

The third key pattern, which is a variation of the previous one with the addition of a spring for each corner of the membrane, has been presented (Fig. 9).

The last proposed key pattern is a system without an elastic membrane or a plate but composed of the piezoelectric patch alone (Fig. 10). The patch is constrained

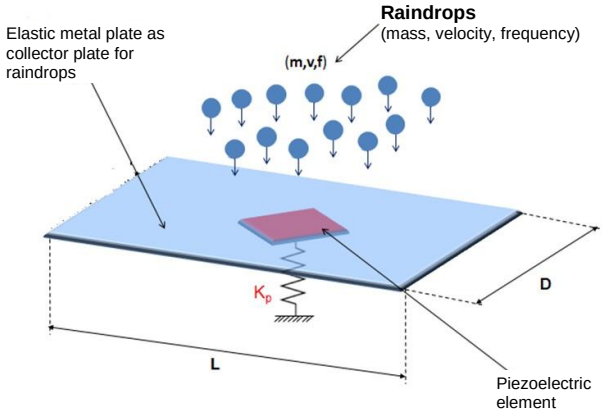

Fig. 8. Ideal concept No.2

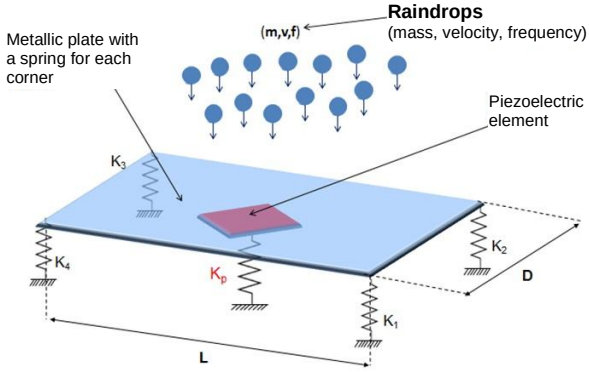

Fig. 9. Ideal concept No.3

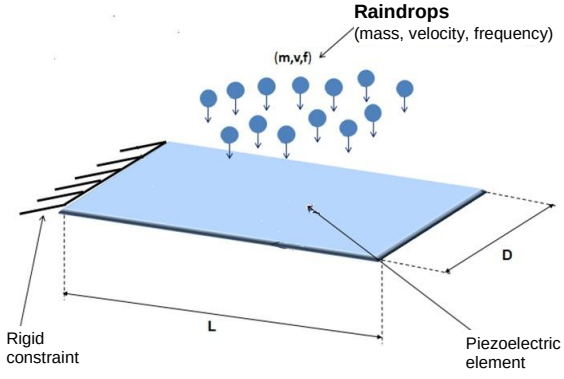

Fig. 10. Ideal concept No.4

on a short side in a fixed way, reproducing the scheme of a cantilever beam. The system, stricken by raindrops, works in a bending way.

Considering the type of load, acting on the harvesting, and the considerations of previous pages, the second and third key pattern results inadequate to the proposed aim. In fact, the slightness of the exciting force, produced by the raindrop's impact, doesn't produce a significant deformation on a stack piezoelectric transducer. As we reported in the first pages, there is a direct relation between the quantity of mechanical energy deformation of piezoelectric unit and the converted one, for this reason the strongly reduced deformation means a negligible conversion of energy by the piezoelectric system. In the market research, reported in the next paragraph, the piezoelectric stack with the smallest axial stiffness presents a value of 12 N/mm with dimensions of 2×3×18 mm and a resonant frequency of 70 kHz.

These considerations, which lead to discarding the second and third configuration, are confirmed by the statements, reported in technical state of art of the first paragraph. In fact, for small loads and for low level of vibrations, Baker, Roundy and Wright (2005) highlight better performance of the 31 mode than 33 mode (the last one is the functionality of the stack configuration).

The first configuration with the glued patch has been discarded too. In fact, the presence of a plate, where the patch is glued, carries to an higher stiffness of the system and consequently to lower deformation in presence of small forces, produced by the impact of raindrop and a very lower energy converted.

At this point, an alternative idea was proposed. Instead of using a plate with a glued piezoelectric patch it is possible to adopt directly a piezoelectric membrane, eliminating in this manner the plate. Also this choice has not been selected for two reasons.

In any way the constraints on all sides of material reduce the deformations of the system, achievable with the presence of a constraint on only one side. Besides, this configuration of a membrane, linked on each side, create a "swimming pool effect". Raindrops amass themselves in the central zone of the membrane, generating a constant deformation. In this manner, the conversion of energy is zero the variation of deformation in the time is necessary because to convert energy in the time.

Finally, for all previous reasons the fourth configuration has been adopted. The literature, as previously seen, support this choice, suggesting the 31 mode as the optimal working mode in the case of low exciting forces. The presence of the piezoelectric patch alone (without any support) and with the minimum number of constraints (only on one side in the cantilever beam configuration) would guarantee the maximum deformations under the low exciting bending actions of raindrops.

4. Choice of piezoelectric material and electro-mechanical model of simulation

After the choice of a key pattern, it is necessary to answer to the question "what is the best material for the final aim?". A market research, involving the main manufacturers of piezoelectric materials has been performed. It carries to fix the attention on two possible types of patches for the cantilever configuration, which is the basic cell-unit of the future "Piezoelectric Shingle" for energy harvesting applications.

The first one is constituted of a piezoceramic Lead Zirconate Titantate PZT material the second one of a polymeric material PolyVinyliDene Fluoride PVDF. After the analysis of the technical datasheets of different piezoceramic PZT materials, built by different manufacturers and different PZT patches, PI DuraAct P.876-A11, constituted of Pic255 material, appears as the most convenient one. The piezoelectric material Pic255 is covered on each side by a layer of a polymeric material, named Kapton. In fact, DuraAct P.876-A11 presents the greatest flexibility for bending loads. This advantage of the greatest bending flexibility is joined to the greater value of electromechanical coupling factor of the material PIC252 than PZT materials of others manufacturers.

The electromechanical coupling factor together with variation of deformation influences the quantity of electrical energy, extracted by a piezoelectric in an application of energy harvesting. Inside the DuraAct family P.876-A11 presents the higher capacity (150 nF) and the smallest bending radius (12 mm).

The same logic process has carried to select the PVDF patch Measurement Specialties LDT1-028K. The selected PVDF patch presents a greater flexibility than PZT P.876-A11 but a smaller electromechanical coupling factor. About these two physical aspects, the two patches follow the general behaviour existing between PZT and PVDF material. The piezoelectric material PVDF is covered on each side by a layer of a polymeric material, named Kapton.

Clearly, a higher flexibility pushes in the direction of a better energetic conversion and the same is made by an higher electromechanical coupling factor. It is necessary to understand inside the selected PZT and PVDF patch, which presents the best tradeoff and consequently the best performance. For this reason, the authors elaborate an electromechanical model to simulate performance of the system about the final energetic conversion for each patch.

The proposed model is composed by three blocks:

– Mechanical model of piezoelectric patch.

– Mechanical model of the raindrop.

– Model for the prevision of the electrical energy converted.

Output data of the blocks 1 and 2 are the input for the third block. In more detail, the block No.1 models the mechanical behaviour of a piezoelectric patch subjected to the action of the impact with a raindrop. In this part of the model, the

Table 1.

Model and Datasheet of PI DuraAct P-876.A11

Technical data	Piezo P-876.A11
Operating voltage	-20 to +200 V
Lateral contraction open-loop	400 μm/m 1,6 μm/(H/mV)
Holding force	90 N
Length/width/thickness	61 mm/35 mm/0.4 mm
Bending radius	12 mm
Piezo ceramic type	Pic 252 – Layer Thickness 100 μm
Electrical capacitance	150 nF

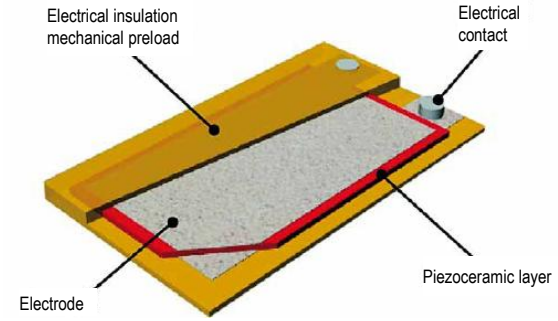

raindrop's impact is modelled with a time history of force applied in the region of impact between the surface of the patch and the raindrop.

For this aim, the FEM approach is used through a software LS-DYNA 971 R4. In this software it builds a FEM mechanical model of the analyzed piezoelectric patch. PZT P.876-A11 is modelled out of 2964 elements of shell type with variable dimensions between 0.5 and 1 mm. Mechanical properties of layers in PIC252 and Kapton materials are adopted in the model, using the formulation of composites in the region of overlapping between Kapton and PIC252. The scheme modelled, is a cantilever beam with a constraint of fixed support on the short side and a free span of 41 mm.

PVDF LDT1-028K is modelled out of 1488 elements of shell type with variable dimensions between 0.5 and 0.9 mm (Fig. 11). Mechanical properties of layers in PVDF and Mylar materials are adopted in the model, using the formulation of composites in the region of overlapping between Mylar and PVDF. The scheme modelled, is a cantilever beam with a constraint of fixed support on the short side and a free span of 31 mm.

The second block of the electromechanical model simulates the raindrop. A FEM model of raindrop is created and it is validated through the results of a previous CFD study also performed by the authors. The CFD analysis uses an approach with VOF (Volume of Fluid) methodology to simulate a multiphase problem as the impact of a raindrop against an infinitely rigid surface. The aim of

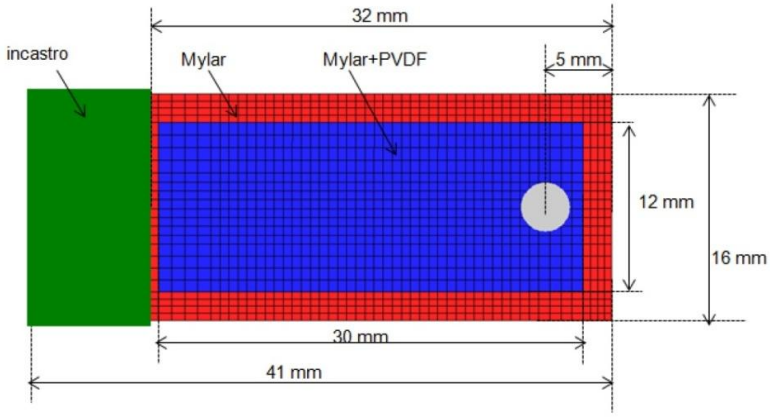

Fig. 11. FEM model of measurement specialties LDT1-028K

CFD study is the evaluation of the impact force of a raindrop against an assigned surface. Then, it will be used as a comparative term to validate the FEM model which is able to calculate deformations of piezoelectric patches and consequently the electric energy achievable.

In the CFD analysis, a 2D and a 3D computational models are built. They are both composed of cells with a dimension of 0,05 mm, considering that the dimension of raindrop falls inside the order of magnitude of some millimeters.

Many simulations have been performed, varying parameters and conditions as the diameter of raindrop, the velocity of impact and the presence or the absence of a water film on the surface. For every case, the result is compared with available experimental data, reported in [36].

It is possible to highlight the similarity of results generated by 2D and 3D model. The numerical results present a lower peak of force than experimental one, but after the first phase of impact their trend matches the experimental one in a good way (see Fig. 12). However, the numerical results give a longer time with higher forces than the experimental ones, for this reason the area under the green rectangle and blue rectangle are similar. For the present problem, the impulse of the force is a fundamental aspect. For this reason, it's possible to affirm that the numerical model gives a good description of experimental phenomena.

Besides, the CFD 3D model is able to show the deformation of raindrop during the impact against the surface (Fig. 13).

After the campaign of simulation with 2D and 3D CFD model, a FEM model of raindrop is built in LS-Dyna software. The FEM model of raindrop is realized using the SPH (Smoothed Particle Hydrodynamics) formulation and it is composed of 11308 SPH elements. These elements are distributed in an uniform manner inside a spherical volume with the diameter of the raindrop. Besides, the elements are linked through the constitutive equations of water, following their formulation, implemented in the LS-Dyna software.

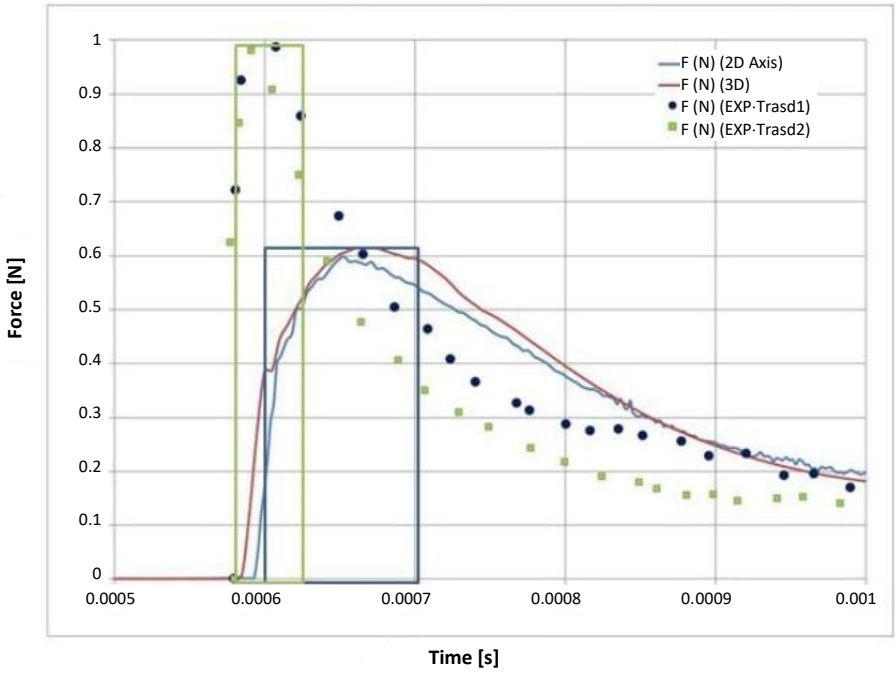

Fig. 12. Results of 2D and 3D CFD models compared with experimental data in the case of a raindrop with a diameter of 3.3 mm and a limit velocity of 8.32 m/s and in absence of water film on the surface

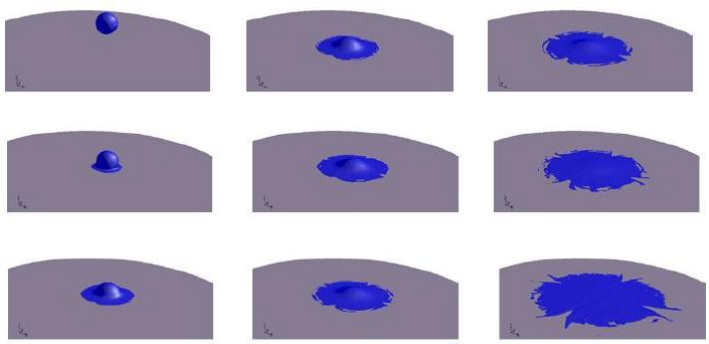

Fig. 13. Deformation of raindrop by the 3D CFD model

The interaction between particles and the main physical dimensions which affect the behaviour of a drop during the impact are calibrated through a comparison with the experimental data and the results of fluid dynamic simulations. In conclusion, the FEM simulation of the impact of a raindrop is validated in the comparison with the experimental approach and the numerical CFD approach.

In Fig. 14 there is reported a global comparison between the three approaches in the case of the impact of a drop with 3.3 mm diameter and with a limit velocity of 8.32 m/s against an infinitely rigid surface. The impact is in absence of a water film on the surface.

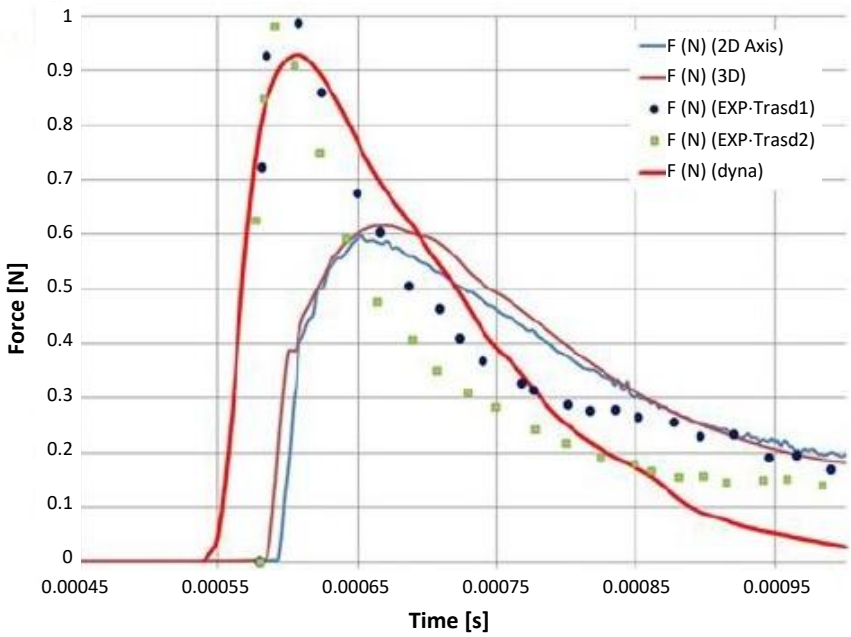

Fig. 14. FEM comparison with experimental data and fluid dynamic numerical results

The FEM model in the peak's region gives a better adherence to experimental data than CFD results. Instead, after the first phase of the impact, in the zone of the decreasing force the FEM curves falls down quicker than experimental data. This model of raindrop is used with the FEM piezoelectric patch model to calculate displacement, strains and the variation of strains in the time of the PZT and PVDF patches (Fig. 15).

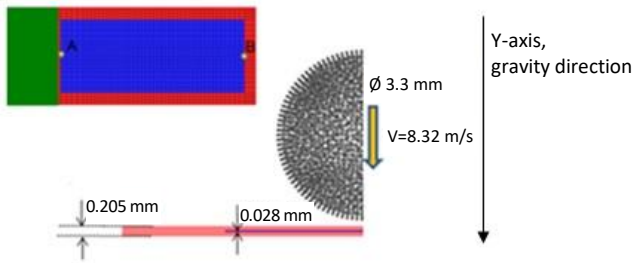

Fig. 15. FEM model of impact between piezoelectric patch and raindrop

Variation of strain for each node in function of the time is the input for the third and last block of the electromechanical model. The third part of the model is addressed to the estimation of the final electric energy converted by a piezoelectric unit after the impact with the drop, simulated in the FEM section of the model. This last section of the model is based on a numerical model, used by Courbon (1988) and implemented in the present activity in an Excel sheet. Equations for the calculation are:

$$U_{elec} = \frac{(K^2 Y \Theta S_{aver}^2)}{2} \tag{9}$$

with: K – coefficient of coupling of the piezoelectric material; Y – Young's modulus of the piezoelectric material; Θ – active volume (is the volume of the piezoelectric material); $S_{aver} = \dfrac{1}{(b-a)} \displaystyle\int_a^b Sr(x_i, t)dx$,

where: $Sr(x_i, t)$ – the difference of strain in the same point but in two consecutive instants of time. Then: $Sr(x_i, t) = S(x_i, t) - S(x_i, t - \Delta t)$; a – initial abscissa (in the longitudinal direction) of the piezoelectric material; b – final abscissa (in the longitudinal direction) of the piezoelectric material; $b - a$ – free length of the piezoelectric material.

Clearly a and b terms depend from the reference system selected in the simulation.

5. Results of simulation campaign

After the presentation of three blocks, composing the electromechanical model, results of a simulation campaign are reported in the present section. Simulations are performed for PVDF LDT1-028K and PZT P.876-A11 both. The first aim of this comparison is the evaluation of the most suitable piezoelectric device for the application proposed.

For the PZT P.876-A11, the subsequent data are inserted in the electromechanical model:

– $K_{31} = 0.351$; $\Theta = l\,w\,t = 150 \cdot 10^{-9}$ m^3; $b - a = 50$ mm $= 0.05$ m;

– Y – Young's modulus $= 62.89 \cdot 10^9$ N/m^2.

For the PVDF LDT1-028K the subsequent data are inserted in the electromechanical model:

– $K_{31} = 0.120$; $\Theta = l\,w\,t = 10.1 \cdot 10^{-9}$ m^3; $b - a = 30$ mm $= 0.03$ m;

– Y – Young's modulus $= 3 \cdot 10^9$ N/m^2.

The simulation case chosen is a raindrop with a diameter of 3.3 mm and a limit velocity of 8.3 m/s, which strikes the piezoelectric surface of PZT and PVDF on the end of the major symmetrical axis in correspondence of their tip. Output of the electromechanical model for the PVDF is reported in the Fig. 16 as electric energy

converted. Then, from energy converted through a derivative operation in the time, an estimation of power is reported.

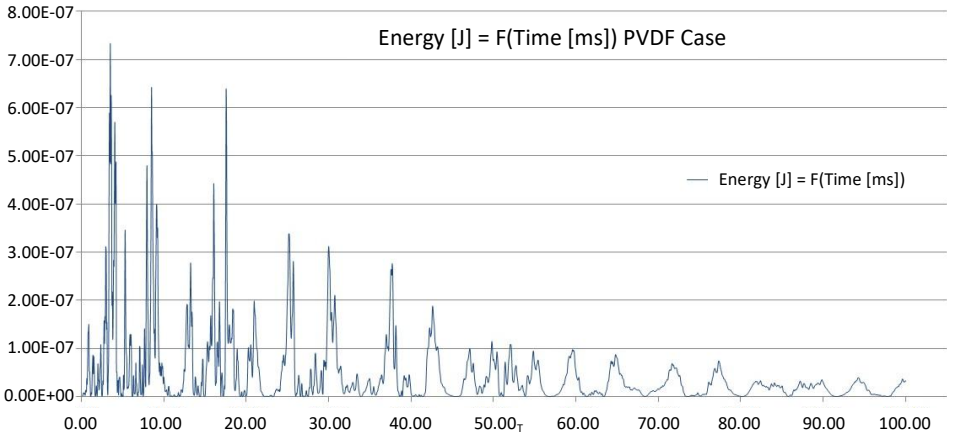

Fig. 16. Electrical energy (J) converted by PVDF patch from an impact with a raindrop with a diameter of 3.3 mm and limit velocity of 8.3 m/s vs time (ms)

The maximum value of energy converted by piezoelectric PVDF during its deformation is 0.73 μJ at 3.5 ms after the beginning of the impact. The maximum power is 6.5 μW (Fig. 17).

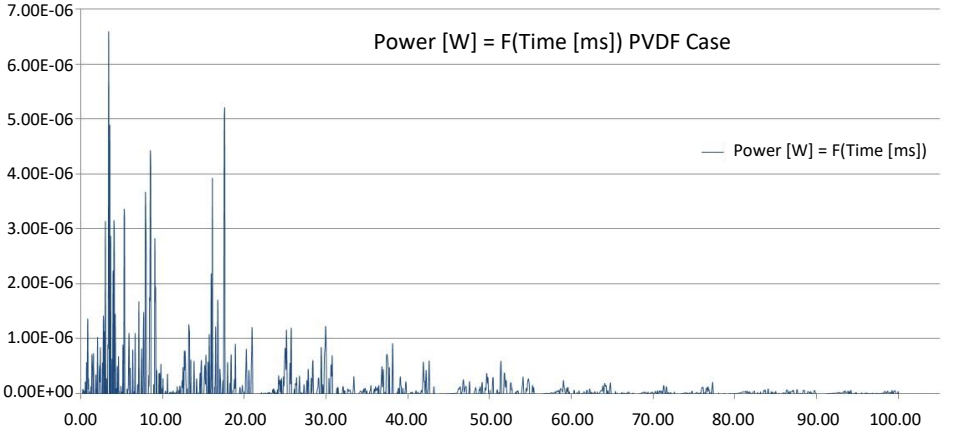

Fig. 17. Power (kW) of PVDF vs time (ms)

The same simulative analysis has been performed for the PZT patch (Fig. 18 and Fig. 19). The maximum value of energy converted by piezoelectric PZT during its deformation is 0.23 μJ at 10.3 ms after the beginning of the impact. The maximum power is 5.8 μW (Fig. 19).

The comparison (Fig. 20) shows that energetic performances of PVDF system are ever better than PZT one.

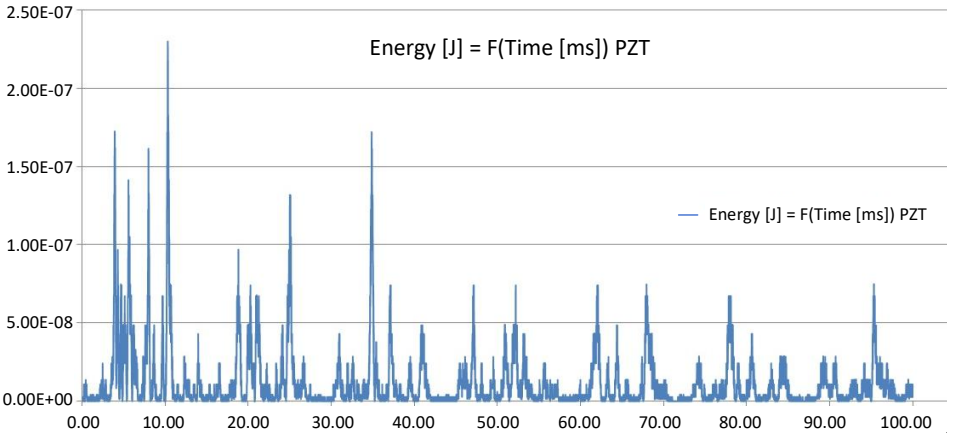

Fig. 18. Electrical energy (J) converted by PZT patch from an impact with a raindrop with a diameter of 3.3 mm and limit velocity of 8.3 m/s vs time (ms)

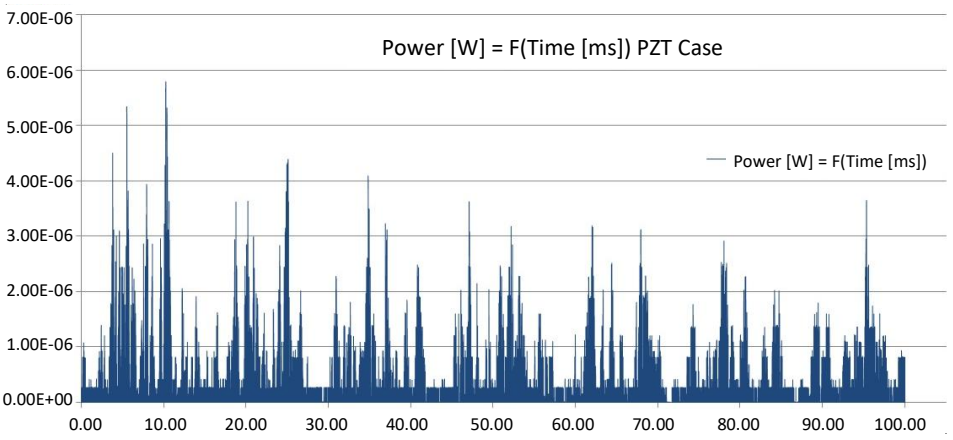

Fig. 19. Power (kW) of PZT vs time (ms)

From the previous data and pictures, it results that the piezoelectric PVDF LDT1-028K has a very great advantageous of performance than PZT P.876-A11. For this reason, the future implementation in the piezoelectric harvesting system, based on rainy precipitations will be based on the PVDF device. This estimation will be also verified in a next work by an experimental point.

PVDF LDT1-028K presents a lower coupling coefficient and a lower active volume than PZT P.876-A11 (a disadvantage for the final performance of the device for energetic conversion) but higher performances. The explanation is in the very greater elasticity of PVDF material than PZT one. In the present study, the exciting force is very low because it is an impact force of a raindrop against a flexible surface. For this reason, the more elastic material present a bigger variation of deformation in the time, then the largest conversion of energy.

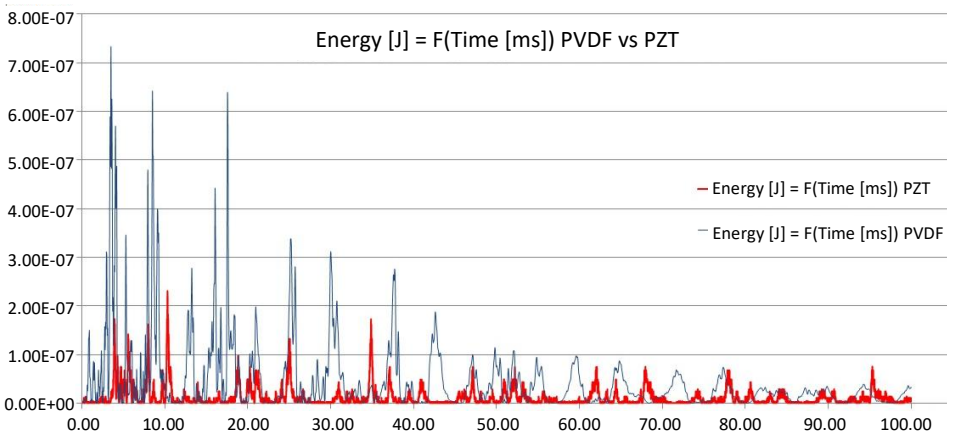

Fig. 20. Comparison of energy converted by PZT (red line) and PVDF (blue line) piezoelectric patches

Besides, PVDF LDT1-028K guarantees other two advantages. The first one is a smaller surface of the device and consequently a greater energy density. The second one is a very lower price compared to the PZT device. This is a fundamental topic for a future realization of a "Piezoelectric Shingle" and an implementation in a roof of a structure to reduce the unitary cost of energy. For this reason, the PVDF patch is more advisable than the PZT one for technical and economical reasons.

6. Conclusions

The present paper has presented a first study on a piezoelectric harvesting system, finalized to obtaining electrical energy from the kinetic energy of rainy precipitation, a renewable energy source not really considered until now. After presenting a state of art of the harvesting systems from environmental energy, linked to vibrations, using piezoelectric structures, and of piezoelectric harvesting systems functioning with rain, the authors have proposed an analysis of the fundamental features of rainy precipitations for the definition of the harvesting system.

Then, four key patterns for the realization of the piezoelectric energy harvesting system have been discussed and analysed, presenting their relative advantages and disadvantages. The final choice is for a cantilever beam scheme, in which the piezoelectric material works in 31 mode.

Then, it has been presented an electro-mechanical model for the simulation of performance of the unit for the energetic conversion, composed of three blocks. The model has been used for a simulation campaign to perform the final choice of the more suitable piezoelectric unit, available on the market, which will be adopted for the realization of the “Piezo Roof Harvesting System”.

The final choice has fallen on a PVDF material for its greater elasticity than the PZT one. In the proposed application, the exciting force is very low because

it is an impact force of a raindrop against a flexible surface. For this reason, the more elastic material present a bigger variation of deformation in time, and then the largest conversion of energy.

Besides, PVDF LDT1-028K guarantees a smaller surface of the device and consequently a greater energy density and a low price. This last point is a fundamental topic for a future realization of a "Piezoelectric Shingle" and an implementation in a roof of a structure to reduce the unitary cost of energy.

Acknowledgements

A thanksgiving is addressed to Evoluzione S.r.l. and Novaetech S.r.l for the courteous support with their competences in this first phase of activity.

Manuscript received by Editorial Board, February 03, 2016;
final version, May 04, 2017.

References

[1] *Annual Energy Outlook 2013*. Report, Energy Information Administration, Washington, DC, USA, 2013.

[2] B.S. Lee, J.J. He, W.J. Wu, and W.P. Shih. MEMS generator of power harvesting by vibrations using piezoelectric cantilever beam with digitate electrode. In *Proceedings SPIE, Smart Structures and Materials 2006: Damping and Isolation*, volume 6169, page 61690B, March, 15 2006. doi: 10.1117/12.658584.

[3] C.S. Lee, J. Joo, S. Han, J.H. Lee, and S.K. Koh. Poly (vinylidene fluoride) transducers with highly conducting poly (3, 4-ethylenedioxythiophene) electrodes. *Synthetic Metals*, 152(1-3):49–52, 2005. doi: 10.1016/j.synthmet.2005.07.116.

[4] F. Mohammadi, A. Khan, and R.B. Cass. Power generation from piezoelectric lead zirconate titanate fiber composites. In *Materials Research Society Proceedings*, volume 736, page D5.5, 2002. doi: 10.1557/PROC-736-D5.5.

[5] H.A. Sodano, J.M. Lloyd, and D.J. Inman. An experimental comparison between several active composite actuators for power generation. In *Proceedings SPIE, Smart Structures and Materials 2004: Smart Structures and Integrated Systems*, volume 5390, pages 370–378, July 26 2004. doi: 10.1117/12.540192.

[6] H.A. Sodano, D.J. Inman, and G. Park. A review of power harvesting from vibration using piezoelectric materials. *Shock and Vibration Digest*, 36(3):197–205, 2004. doi: 10.1177/0583102404043275.

[7] H.A. Sodano, G. Park, and D.J. Inman. Estimation of electric charge output for piezoelectric energy harvesting. *Strain*, 40(2):49–58, 2004. doi: 10.1111/j.1475-1305.2004.00120.x.

[8] J. Baker, S. Roundy, and P. Wright. Alternative geometries for increasing power density in vibration energy scavenging for wireless sensor networks. In *3rd International Energy Conversion Engineering Conference*, page 5617, San Francisco, CA, USA, 16-18 August 2005. doi: 10.2514/6.2005-5617.

[9] S. R Platt, S. Farritor, and H. Haider. On low-frequency electric power generation with PZT ceramics. *IEEE/ASME Transactions on Mechatronics*, 10(2):240–252, 2005. doi: 10.1109/TMECH.2005.844704.

[10] T.H. Ng and W.H. Liao. Sensitivity analysis and energy harvesting for a self-powered piezoelectric sensor. *Journal of Intelligent Material Systems and Structures*, 16(10):785–797, 2005. doi: 10.1177/1045389X05053151.

[11] S. Roundy. On the effectiveness of vibration-based energy harvesting. *Journal of Intelligent Material Systems and Structures*, 16(10):809–823, 2005. doi: 10.1177/1045389X05054042.

[12] D. Benasciutti, E. Brusa, L. Moro, and S. Zelenika. Optimised piezoelectric energy scavengers for elder care. In *Proceedings of European Society Precision Engineering & Nanotech (EUSPEN) Conference*, pages 41–45, Zurich, Switzerland, May 2008.

[13] L. Mateu and F. Moll. Optimum piezoelectric bending beam structures for energy harvesting using shoe inserts. *Journal of Intelligent Material Systems and Structures*, 16(10):835–845, 2005. doi: 10.1177/1045389X05055280.

[14] K. Mossi, C. Green, Z. Ounaies, and E. Hughes. Harvesting energy using a thin unimorph prestressed bender: geometrical effects. *Journal of Intelligent Material Systems and Structures*, 16(3):249–261, 2005. doi: 10.1177/1045389X05050008.

[15] M. Ericka, D. Vasic, F. Costa, G. Poulin, and S. Tliba. Energy harvesting from vibration using a piezoelectric membrane. In *Journal de Physique IV (Proceedings)*, volume 128, pages 187–193, September 2005. doi: 10.1051/jp4:2005128028.

[16] S. Kim, W. W Clark, and Q.M. Wang. Piezoelectric energy harvesting with a clamped circular plate: analysis. *Journal of intelligent Material Systems and Structures*, 16(10):847–854, 2005. doi: 10.1177/1045389X05054044.

[17] S. Kim, W. W Clark, and Q.M. Wang. Piezoelectric energy harvesting with a clamped circular plate: experimental study. *Journal of Intelligent Material Systems and Structures*, 16(10):855–863, 2005. doi: 10.1177/1045389X05054043.

[18] J. Han, A. von Jouanne, T. Le, K. Mayaram, and T.S. Fiez. Novel power conditioning circuits for piezoelectric micropower generators. In *Applied Power Electronics Conference and Exposition, 2004. APEC'04. Nineteenth Annual IEEE*, volume 3, pages 1541–1546, 2004. doi: 10.1109/APEC.2004.1296069.

[19] E. Lefeuvre, A. Badel, C. Richard, L. Petit, and D. Guyomar. A comparison between several vibration-powered piezoelectric generators for standalone systems. *Sensors and Actuators A: Physical*, 126(2):405–416, 2006. doi: 10.1016/j.sna.2005.10.043.

[20] A. Preumont. *Mechatronics. Dynamics of Electromechanical and Piezoelectric Systems*, volume 136. Springer, 2006. doi: 10.1007/1-4020-4696-0.

[21] R. Guigon, J.J. Chaillout, T. Jager, and G. Despesse. Harvesting raindrop energy: theory. *Smart Materials and Structures*, 17(1):015038, 2008. doi: 10.1088/0964-1726/17/01/015038.

[22] R. Guigon, J.J. Chaillout, T. Jager, and G. Despesse. Harvesting raindrop energy: experimental study. *Smart Materials and Structures*, 17(1):015039, 2008. doi: 10.1088/0964-1726/17/01/015039.

[23] P.V. Biswas, M.A. Uddin, M.A. Islam, M.A.R. Sarkar, V.G. Desa, M.H. Khan, and A.M.A. Huq. Harnessing raindrop energy in Bangladesh. In *Proceedings of the International Conference on Mechanical Engineering*, Dhaka, Bangladesh, 26-29 December 2009. Paper: ICME09-AM-29.

[24] J.S. Marshall and W. Mc K. Palmer. The distribution of raindrops with size. *Journal of Meteorology*, 5(4):165–166, 1948. doi: 10.1175/1520-0469(1948)005<0165:TDORWS>2.0.CO;2.

[25] J.S. Marshall, R.C. Langille, and W. Mc K. Palmer. Measurement of rainfall by radar. *Journal of Meteorology*, 4(6):186–192, 1947. doi: 10.1175/1520-0469(1947)004<0186:MORBR>2.0.CO;2.

[26] J.O. Laws and D.A. Parsons. The relation of raindrop-size to intensity. *Eos, Transactions American Geophysical Union*, 24(2):452–460, 1943. doi: 10.1029/TR024i002p00452.

[27] J.W. Ryde. The attenuation and radar echoes produced at centimetre wave-lengths by various meteorological phenomena. In *Report of a conference on Meteorological factors in radio-wave propagation*, pages 169–188, The Physical Society and the Royal Meteorological Society, London, 8 April 1946.

[28] A.C. Best. The size distribution of raindrops. *Quarterly Journal of the Royal Meteorological Society*, 76(327):16–36, 1950. doi: 10.1002/qj.49707632704.

[29] R. S Sekhon and R.C. Srivastava. Doppler radar observations of drop-size distributions in a thunderstorm. *Journal of the Atmospheric Sciences*, 28(6):983–994, 1971. doi: 10.1175/1520-0469(1971)028<0983:DROODS>2.0.CO;2.

[30] P.T. Willis. Functional fits to some observed drop size distributions and parameterization of rain. *Journal of the Atmospheric Sciences*, 41(9):1648–1661, 1984. doi: 10.1175/1520-0469(1984)041<1648:FFTSOD>2.0.CO;2.

[31] G. Feingold and Z. Levin. The lognormal fit to raindrop spectra from frontal convective clouds in Israel. *Journal of Climate and Applied Meteorology*, 25(10):1346–1363, 1986. doi: 10.1175/1520-0450(1986)025<1346:TLFTRS>2.0.CO;2.

[32] D. Sempere-Torres, J.M. Porrà, and J.D. Creutin. A general formulation for raindrop size distribution. *Journal of Applied Meteorology*, 33(12):1494–1502, 1994. doi: 10.1175/1520-0450(1994)033<1494:AGFFRS>2.0.CO;2.

[33] D. Sempere-Torres, J.M. Porrà, and J.D. Creutin. Experimental evidence of a general description for raindrop size distribution properties. *Journal of Geophysical Research: Atmospheres*, 103(D2):1785–1797, 1998. doi: 10.1029/97JD02065.

[34] K.V. Beard and H.R. Pruppacher. A determination of the terminal velocity and drag of small water drops by means of a wind tunnel. *Journal of the Atmospheric Sciences*, 26(5):1066–1072, 1969. doi: 10.1175/1520-0469(1969)026<1066:ADOTTV>2.0.CO;2.

[35] G. Montero-Martínez, A.B. Kostinski, R.A. Shaw, and F. García-García. Do all raindrops fall at terminal speed? *Geophysical Research Letters*, 36(11), 2009. L11818, doi: 10.1029/2008GL037111.

[36] M.A. Nearing, J.M. Bradford, and R.D. Holtz. Measurement of force vs. time relations for waterdrop impact. *Soil Science Society of America Journal*, 50(6):1532–1536, 1986. doi: 10.2136/sssaj1986.03615995005000060030x.